Data Processing for the DENIS project

E.R. DEUL[1], A. HOLL[1,7], F. GUGLIELMO[1,3], J. BORSENBERGER[2], E. BERTIN[2], B. DE BATZ[3], E. COPET[3], N. EPCHTEIN[3], P. FOUQUÉ[3], F. LACOMBE[3], T. LE BERTRE[3], D. ROUAN[3], S. RUPHY[3], D. TIPHÈNE[3], S. KIMESWENGER[4], C. KIENEL[4], J. HRON[5], T. FORVEILLE[6]

[1] *Leiden Observatory, Leiden, Netherlands*
[2] *Institut d'Astrophysique de Paris, France*
[3] *Observatoire de Paris, France*
[4] *Astronomische Institute, Innsbruck, Austria*
[5] *Sternwarte Wien, Vienna, Austria*
[6] *Observatoire de Grenoble, Grenoble, France*
[7] *Konkoly Observatory, Budapest, Hungary*

ABSTRACT. The Data Processing Pipeline of the DENIS project is described in some detail. The emphasis is directed toward the implemented and planned reduction algorithms and to the considerations that lead to their choice. The two major topics dealt with here are the astrometric and photometric calibrations of the DENIS project.

1. Introduction

The DENIS project is the first attempt to create a digitized map of a large surface of the sky in the Near–Infrared range. This contribution mainly concentrates on the technics and methods of data processing that are currently being implemented in the dedicated data analysis centers. A more detailed description of the DENIS scientific objectives and focal instrument hardware can be found in Epchtein et al.(1994) or in the so called DENIS Blue Book (Epchtein et al. edts., 1994), but the main baselines of the project and its present status is briefly summarized in this introduction.

DENIS aims at mapping the all southern sky in 3 bands of the near–infrared range (I, J and K_s) at arcsecond spatial resolution. This survey is performed simultaneously in 3 colours with a specially designed camera attached at the cassegrain focus of the 1 meter telescope of the European Southern Observatory at La Silla, Chile. The limiting magnitudes currently achieved during the presently on–going commissioning phase *(protosurvey)* are 16 and 14 in J and K_s, respectively at 3 σ with a standard integration time of 10 seconds. The I camera is in the final stage of testing in the laboratory and the survey is planned to start as soon as this third channel will be set–up and tested on the telescope. The full coverage of the southern sky will last for about 4 years.

The data processing required for the creation of the DENIS final products involves several stages that can be mapped to geographical locations. The first location is on La Silla where the actual data acquisition and preprocessing steps take place. Aspects of these steps will be discussed in section 2. The preprocessed data are forwarded to the next processing center in the pipeline; the Paris Data Analysis Center (PDAC). For a

more detailed description of the processing algorithms involved in the flat fielding and image corrections taking place at PDAC see Borsenberger et al, 1995. Upon successful PDAC processing the DENIS data are forwarded to the Leiden Data Analysis Center (LDAC). There the small source extractions are done and the astrometric and photometric calibrations are performed. Both these calibration steps are discussed in some detail in sections 3 and 4. For more detail on the source extraction algorithm see Deul (1994),

2. On Site Processing

The major processing tasks on the observing site are performed by two units. These are the Real Time Unit (RTU) responsible for acquiring the data and preprocessing it for transport, and the Non Real Time Unit (NRTU) which controls the whole acquisition and administration process.

2.1. The RTU

The major tasks of the RTU in terms of data processing are the acquisition of data and the preprocessing of that data to allow flexible and compressed transport to the other Data Processing Centers (DACs). Preprocessing of the data stream is aimed at allowing quality control on site and to obtain high loss-less compression ratios for storing the data on transport tapes.

By means of sliding-window median filtering of frames from observed strips the individual strip frames are provisionally flat fielded, sky subtracted and bias corrected to obtain 'flat' images that can be compressed at high ≥ 2 ratios. This provisional processing is completely reversable to allow the PDAC to recreate the original raw data.

In addition the RTUs perform simple source extractions at varying levels of accuracy to allow the NRTU to check different observational conditions such as focus, photometric, and pointing accuracies.

Figure 1 shows a schematic view of the RTU configuration.

2.2. The NRTU

The NRTU provides the binding between the Focal Instrument and its controlling and preprocessing units (RTUs) on one side and the Observer, the ESO telescope, and the DACs on the other side (see Figure 2). The NRTU is designed to prepare the observations schedule (see Kimeswenger and Kienel, 1994), control the data acquisition, and the general data stream. In addition it analyses the results of the online preprocessing.

On-line data analysis is done by means of dedicated tasks that provide automatized on site decision mechanisms and prepare the information for the observers display (see Figure 3). Several tasks are run to check the performance of the data acquisition system.

The `astrometric correction task` is using raw source extractions provided by the RTU preprocessing tasks and performs a pattern matching algorithm with stars from the HST Guide Star Catalogue (Jenkner et al., 1990). This algorithm is based on

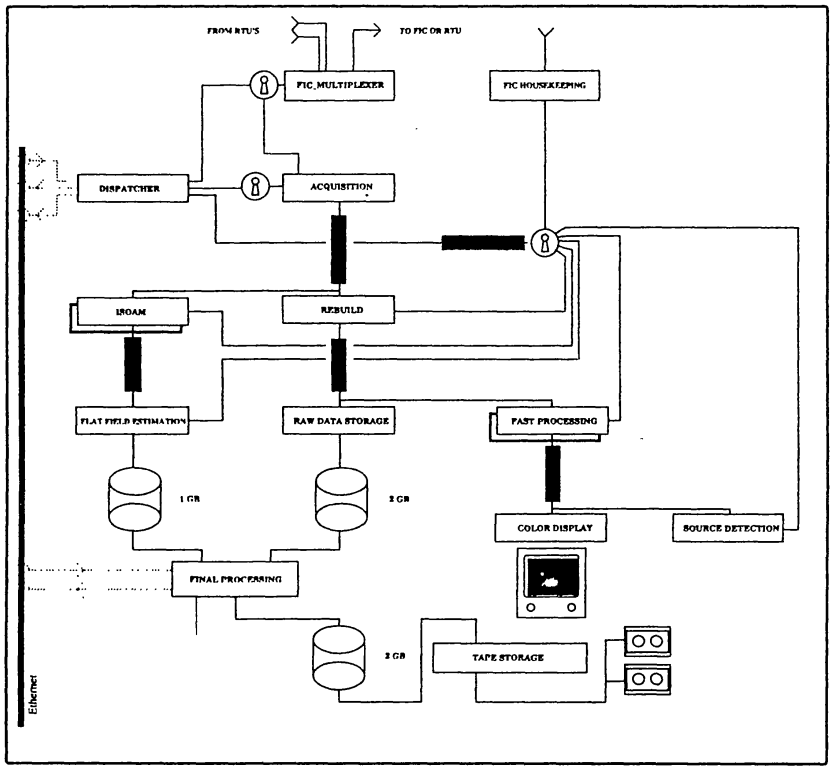

Fig. 1. Schematic view of the RTU configuration

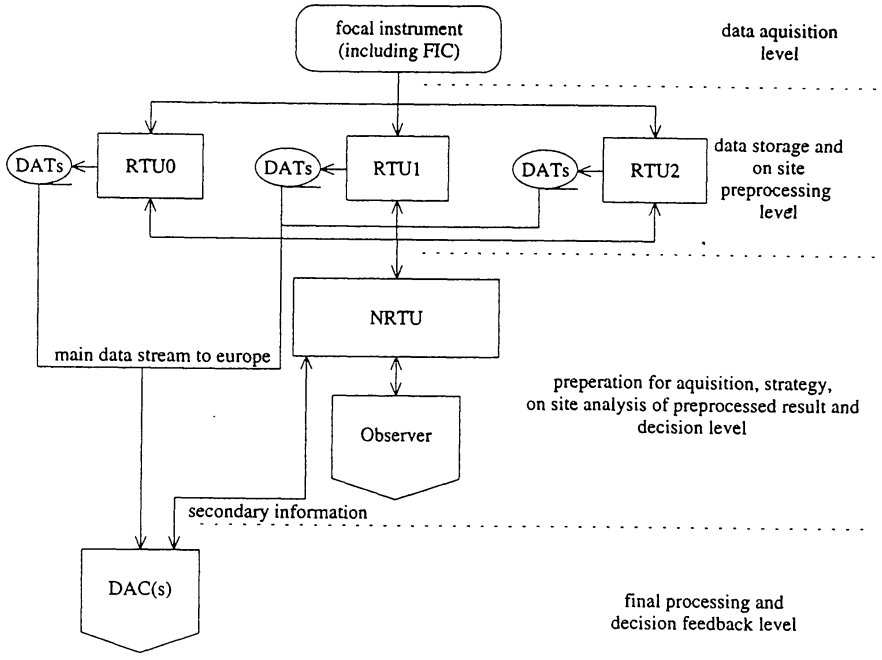

Fig. 2. Role of the NRTU in the data acquisition chain

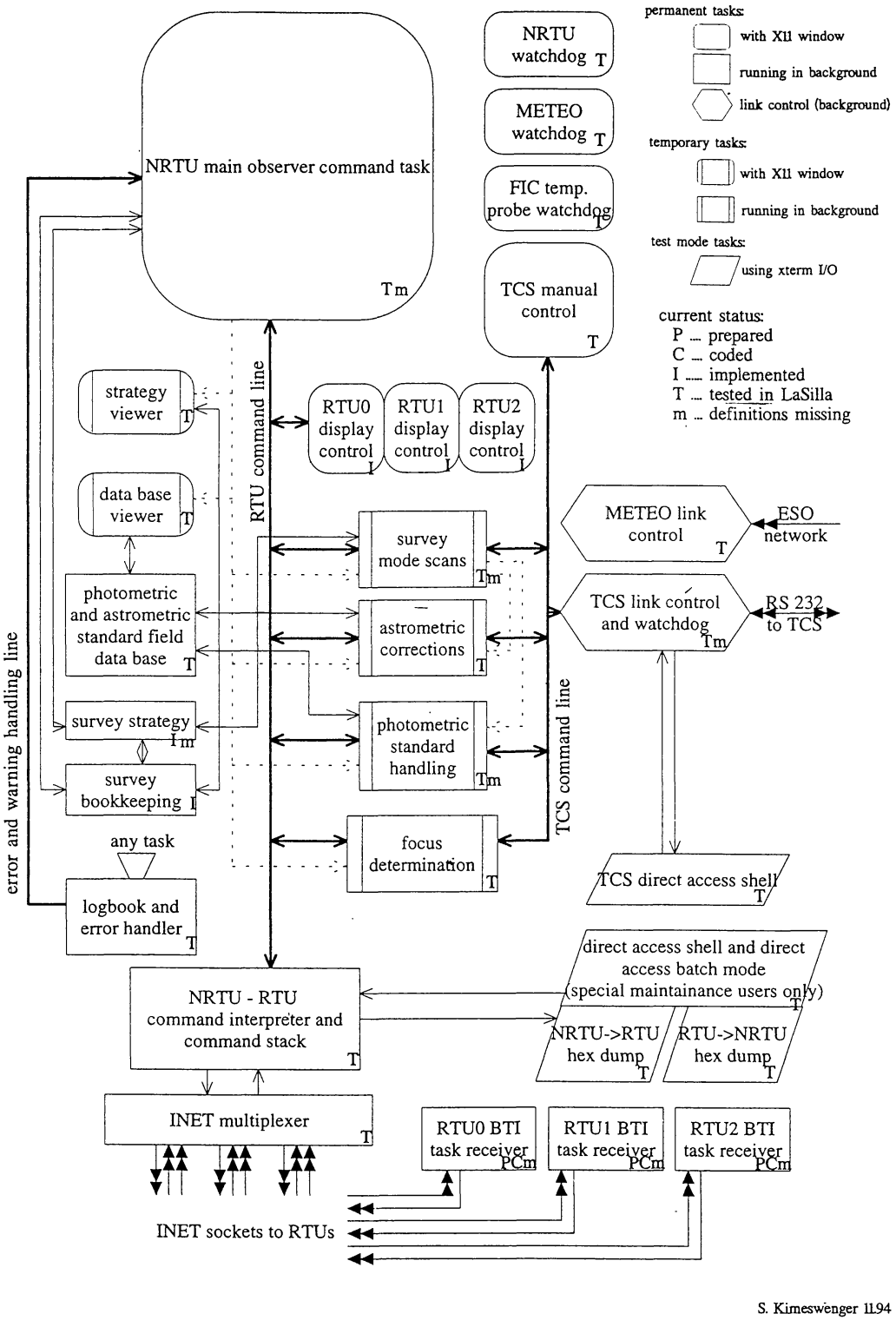

Fig. 3. Overview of NRTU tasks

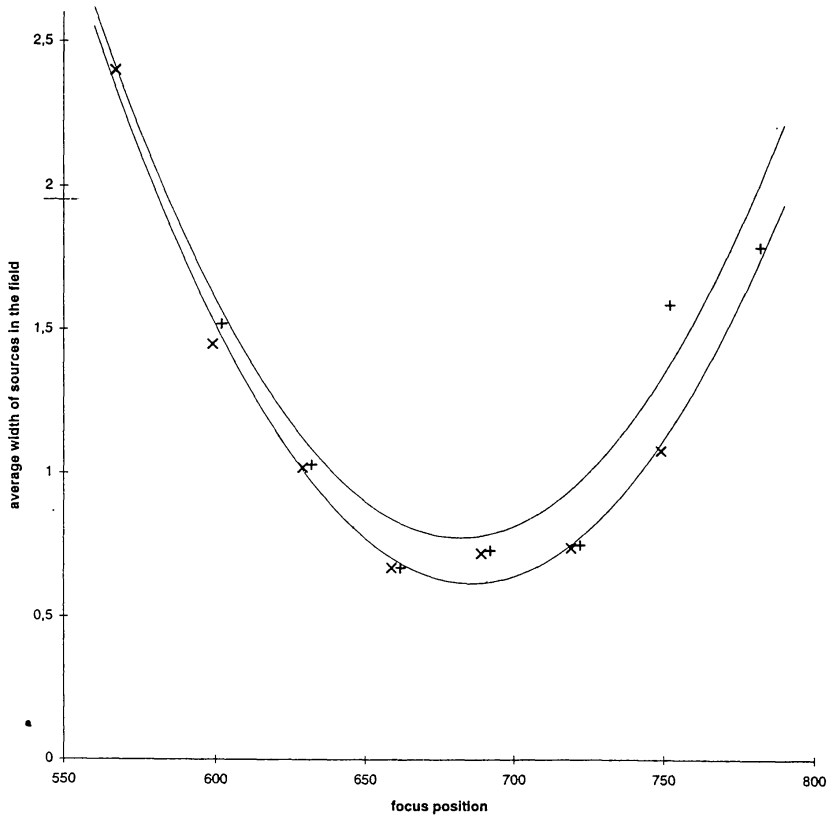

Fig. 4. Focussing curve

a boxcar search function in cylindrical (r, φ) coordinates and assumes, that the image distortion and the rotation are approximately know (see section 3.2). The results are used to correct the telescope coordinate system during observations, are displayed at real time, and are reported (via electronic logbook) to the DACs.

The `photometric standard handling task` is using a more accurate mode of the RTU preprocessing source extraction on photometric standards. The photometric standards database used (see section 4.1) includes more than 150 standard stars. The lower order extinction coefficients are derived and the higher order extinction coefficients are taken from feedback by the DACs. These low order coefficient must be set by the observer as this needs human interaction/decisions.

The `focus determination and control task` uses again the more accurate mode of the RTU preprocessing source extraction. It optimizes the focus. Because the 3 arcsec pixels undersample the PSF, the information of slightly defocused images at both sides from the best focus is used to obtain the central position of the focal plane (see Figure 4).

The `survey mode scan task` uses periodically determined sky background levels and noise values to determine variations of the meteorological conditions. In addition the quality of the PSF width is monitored.

3. Astrometric Calibration

A first-order position reconstruction is obtained through a pre-astrometric phase that reliably cross-identifies extracted objects with a reference astrometric catalog, discussed

in section 3.1. After this identification has been made, improved estimates of the telescope pointing, plate scale and distortion, are obtained by least square adjustment to the known absolute positions of these reference sources (see section 3.4 and further).

For each frame we determine independent pointing offsets, while still considering the focal scale and distortion parameters as constant or smoothly variable at the strip level. For the sake of simplicity they are presently described as Chebychev polynomials of the frame number.

3.1. The Input Catalog

The original raw DENIS data consist of frames (telescope pointings) with positions reported by the encoders of the telescope and the telescope control system. Although the ESO 1m telescope encoders have a 1" step, the pointing error is in the order of 5", possibly limiting the potential position accuracy of the DENIS survey. The source extraction algorithm produces lists of objects on each frame with an accuracy of at least 0.1" for bright sources. To remove this unnecessary limitation, independent pointing offsets are determined for each frame, and at a later stage allow for focal scale and plate distortion.

To derive such pointing values a reference catalogue is required that has an average density of at least a few reference stars per frame amounting to a minimum size of a few million stars for the southern hemisphere. This requirement leaves only one candidate from the usual astronomical catalogs (AGK3, SAO, PPM,...): the Guide Star Catalog (GSC) from the Hubble Space Telescope. It consists of about 19 million entries (for both hemispheres), of which roughly 15 million are classified as stellar. The non-stellar entries are optically imperfect stars (near the plate edges), such as blends, galaxies, nebulae, that have less accurate and possibly color-dependent positions. The remaining 15 million stars should be detectable to I=18 mag (the completeness limit for the southern part of the GSC is about B=15). Their number lies well above our minimum requirement and provides a good basis for a positional reference grid.

The errors of the present GSC version are about 1-2" (Taff et al., 1990) and are dominated by systematic effects. The relative, short distance position differences are accurate up to 0.4 - 0.8" rms. The next version, to be released in 1995, should have the systematic part removed and have a roughly uniform and uncorrelated standard error of 0.5"; which might degrade to 1" at plate corners (this does not include proper motions) (Lasker, 1995). The average of 20 years between the earliest GSC input plates and the DENIS survey requires corrections for proper motions. The corrections for known high proper stars will be applied using the PPM catalog as the reference catalog.

The DENIS input catalog (ICAT) was created from the 8.5 million stellar entries south of declination +7.5 deg. For those objects that have multiple entries in the GSC the positions have been averaged. From the original GSC field entries only the identifiers, coordinates and magnitude values have been retained. The ICAT is divided into cells of 20' by 20', and the contents of those cells can be accessed through a hashing table. Statistical analysis of the ICAT shows that on average each DENIS frame we will have 15 GSC stars. There will be more than 4 thousand frames without a GSC star; about 25000 frames will have only one or two star.

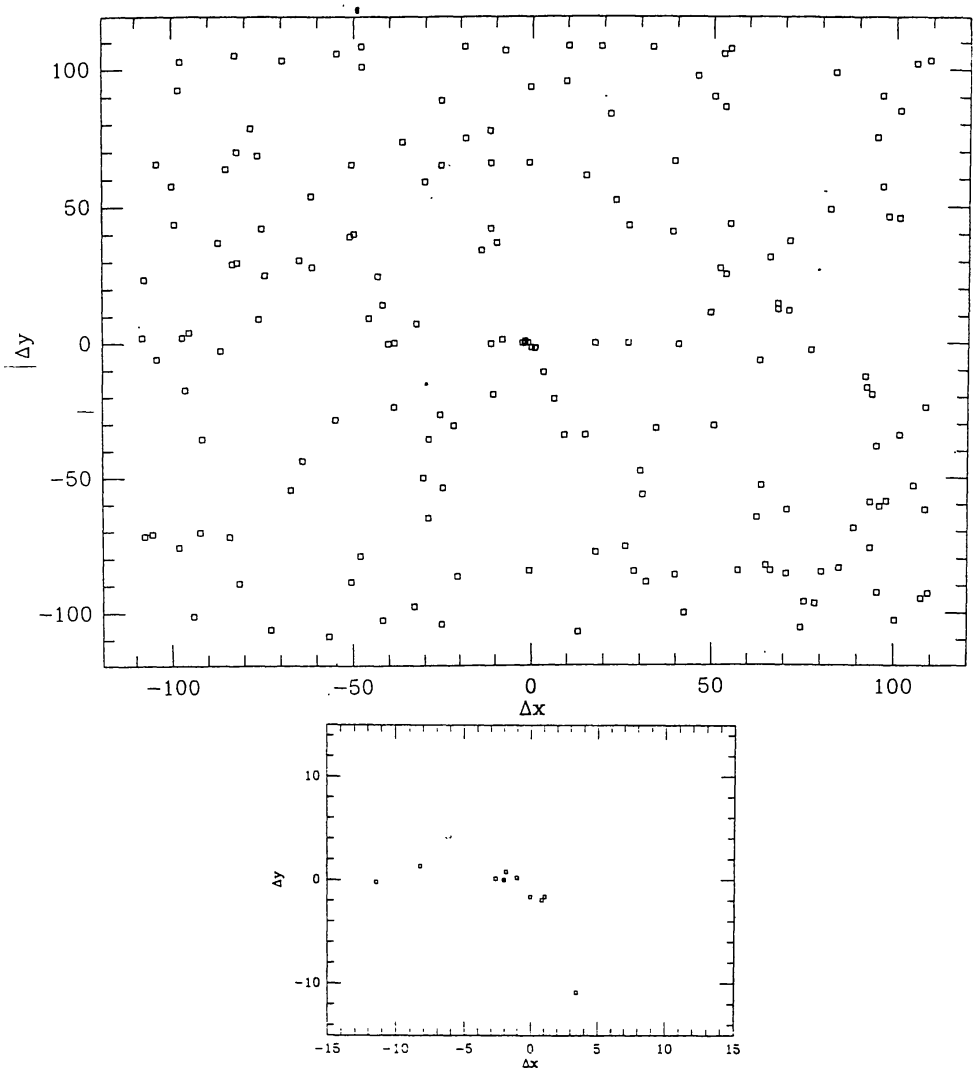

Fig. 5. Example of a typical coordinate differences plane

The accuracy of the ICAT can be improved by the introduction of the TYCHO catalog of the HIPPARCOS satellite. The TYCHO objects will have much better positional accuracy (0.03" rms, Høg et al., 1991), but will contain only about 1 million stars (on average one star every other DENIS frame).

3.2. Frame offsets and object pairing

For each frame in a strip the list of ICAT stars and the list of extracted raw objects are used to determine the pairing between these lists. This is done by stepping along the list of reference objects (ICAT stars), and using a sliding window algorithm, to select those objects in the right ascension-ordered list of the extracted objects that are within a given error box. The coordinate differences are used to derive the frame offset. Whenever there is a pattern match between the ICAT stars and the extracted objects, this results in a concentration of coordinate differences in the plane of pixel position differences (see Figure 5). In case of too few stars in the pattern, or when there is no pattern match, the plane of pixel position differences will be filled in a Poissonian way. The concentration of coordinate differences is found by means of a boxcar peak searching algorithm. The statistical significance of the determination is tested.

3.3. The pre-astrometric processing pipeline

The pre-astrometric phase of the processing pipeline starts with trying to lock on the position of the first frame of the given strip. This is necessary because the positional accuracy of the telescope pointing degrades with longer slew distances. The ICAT objects of a large (about 30' by 30') area of the sky are obtained, and offsets between the GSC stars with extracted objects are derived. Then shifting the coordinates of the extracted objects with the derived offset value, they are paired with GSC stars. The thus derived frame position is necessarily less accurate than what is required or can be achieved with better initial position information. Therefore, this process is repeated until in-strip accuracy is reached with smaller search windows. In case there are more objects within the minimum required distance the brightest is chosen.

To step over frames where no correct matching can be achieved between the ICAT stars and extracted objects, a running average of frame offsets is used to extrapolate the systematic offset behaviour across such gaps.

In conjunction with the single frame position determination, the offset between two consecutive frames is independently derived, using the stars in their overlap region. Using these offsets the overlap stars are paired. Finally the objects from the three different channels are paired as well, after their offsets have been determined.

This way we get three independent estimates for the frame center positions: an absolute one through the pairing with GSC stars, and relative ones through pairings with the previous frame and with the other channels. The associated lists: the pairing information (DENIS vs. GSC, DENIS vs. DENIS in the overlap region, DENIS vs. DENIS at the different channels) and the derived frame offsets are the input to the astrometry program.

3.4. Plate model of least squares solution

The obtain reliable positions through least squares determination a plate model is defined as the mapping between pixel coordinates and the so-called normal coordinates. These normal coordinates (ζ, η) are the gnomonic projection of the absolute sky positions relative to the field center. There is some level of non-linearity here, since the field center itself depends on the position reconstruction, but for realistic initial errors this is very small and easily absorbed in the plate model.

3.5. Overlap solution

The density of the Input Catalog is almost always sufficient to allow determination of the frame offsets. There are, however, many frames ($\approx$12500) where no reliable offset determination can be derived. Fortunately, the DENIS fields have sufficient overlap (2' on each side), and dark clouds are sufficiently transparent at K, that in most cases some stars will be detected in the overlap. They are used to extend the reference system.

The coefficients of the plate model will thus be determined by simultaneously minimizing (in a least square sense) the distance to the reference stars and the overlap detections.

3.6. Intercolor Mapping

Even though the discussion in the previous sections is based on processing of a single channel, this is mainly for illustrative purposes and it is easily generalised to simultaneous processing of the three channels. The three images of one field are then considered as a case of (nearly total) overlap, and the plate model is generalized to include one set of parameter per colour. The only significant difference is that the pointing centers for the three colours are not independent random parameters: the encoder readout error is the same for all colours, and only the smoothly varying flexures are independent. This is most easily handled by describing the pointing center of one reference channel as an independent variable for each field, and the offsets between the reference channel and the other two as a smoothly varying function of the field number.

3.7. Implementation of the least squares solver

We consider here an ensemble of n_f fields containing a total of N_{ref} reference stars and N_{over} stars in overlaps, and adjust a plate model which has n_{par} smoothly varying functions (such as the polynomials discussed above) with coefficients noted as b_p, plus one zero point per field noted as b_f.

For a practical discussion of the implementation, it is convenient to write the quadratic least squares equation under its canonical form

$$S = (A \cdot X - B)^T \cdot (A \cdot X - B) \tag{1}$$

where A is a rectangular matrix (the design matrix) whose dimensions are the total number of constraints (reference+overlap) and the total number of fitted coefficients (field centers+smooth functions). X and B are vectors containing respectively the fitted coefficients and the constraints data.

Under this canonical formulation of the least square quadratic form, it is easy to show (see for instance the least square chapter in Numerical Recipes) that the X which minimises the errors is the solution of the system of $(n_{par} + n_f)$ linear equations $(A^T \cdot A) \cdot X = A^T B$, known as the normal equations.

The plate model coefficients can thus be obtained by computing $(A^T \cdot A)$ and solving the normal equations. This method is generally known to have relatively poor numerical stability. Once the pixel coordinates are remapped to [-1,1] however, the problem has good conditioning, and direct comparison with more accurate methods shows good agreement for modest polynomial degrees, even in single precision. Alternatively, A is sparse enough that solving the equation with the conjugate gradient algorithm is a possibility. This iterative minimisation algorithm converges in at most $n_{par} + n_f$ steps, each of which needs one multiplication by A and its transpose. It has good stability, is about as fast as computing $(A^T \cdot A)$, but needs a larger memory space. If on the other hand an analytic estimate of the standard errors is needed, $(A^T \cdot A)^{-1}$ (which is the covariance matrix) must be evaluated anyway. Solving the normal equations then becomes much cheaper, though we may still use the conjugate gradient for the minimization, because of its better numerical behaviour.

3.8. Error estimate

It is possible to obtain an analytical derivation for the position standard error involved in solving above least squares problem. This error is easily evaluated for "semi-global" (strip-wide) reduction, but it cannot be used for truly global processing of the full survey. The size of the covariance matrix is then larger than $10^6 x 10^6$, and the computation becomes impractical. Also, the analytic expression cannot be generalized to the case of correlated errors, and the errors in the GSC have a strong systematic component. The only practical method to deal with correlated errors is Monte-Carlo simulation: several realisation of the appropriate probability distribution are added to the input parameters (here the catalog position and measurements of the reference stars), and comparison of the corresponding solutions with the nominal one is used to estimate its uncertainty. As always with Monte-Carlo methods, the main drawback is the slow convergence of the estimate, whose relative accuracy is the square root of the number of trials. However, what is estimated here is an error, and utmost accuracy is certainly not needed. If we can contend with 30% accuracy, only 10 samplings are needed, which would probably be feasible for the full sky, and could cope with systematic error if their characteristic scale is approximately known.

After running the astrometry program, pre-astrom can be iterated once more, using smaller error boxes, achieving better pairing this way. This can be done because the full astrometric solution from the least square solution provides better estimates for the plate model parameters and identifies possible mismatches in the pre-astrometric pairing. After this the least squares solution can be run once more with higher reliability.

3.9. Timing and accuracy

Given the scale of the data reduction effort in DENIS, attention was given to processing power requirements as well as to accuracy. The timings displayed below have been measured on an IBM RS6000/320. They are strict upper limits. One can realistically hope that the systematic errors of the GSC get smoothed to some extent in the solution, out to this scale of about 3 fields. We have also checked that the accuracy of the solution isn't significantly degraded for a single field without reference stars. A three field gap on the other hand doubles the errors for the middle field.

3.10. Full sky processing

There is conceptually no great difference between cross-strip and in-strip overlaps, except that cross strip overlaps involve a different set of distortion constants. However, the cpu timing for the above algorithm roughly scales as the square of the number of simultaneously processed fields, and brute force application to the full sky (one million fields) is thus clearly impossible. Fortunately, the problem has a very local structure, and should lend itself well to iterative methods. After the first strip-based solution, we plan to consider all stars in the overlapping strips as additional reference stars, using the current plate parameters to compute their positions.

N_{star}	N_{ref}	σ_{ref}	σ_{mes}	p_{deg}	f_{deg}	t_{cpu}	σ_{sys}
100	15	0.45	0.45	1	0	196	0.06
100	15	0.45	0.45	2	0	363	0.06
100	15	0.45	0.45	3	0	706	0.06
100	15	0.45	0.45	4	0	1219	0.06
100	15	0.45	0.45	1	1	317	0.06
100	15	0.45	0.45	2	1	858	0.06
100	15	0.45	0.45	3	1	1872	0.06
100	15	0.45	0.45	4	1	4414	0.07
100	15	0.45	0.45	1	2	482	0.06
100	15	0.45	0.45	2	2	1467	0.06
100	15	0.45	0.45	3	2	3799	0.06
100	15	0.45	0.45	4	2	11620	0.07
100	15	0.45	0.45	1	3	684	0.06
100	15	0.45	0.45	2	3	2461	0.06
100	15	0.45	0.45	3	3	8149	0.07
100	15	0.45	0.45	4	3	16487	0.08

Multicolour solution

3.11. Results for actually observed strips

The following strips, observed at the end of 1994, have been fully processed:

Strip Number	α	δ
601	331°.6	+2°→−27°.5
605	075°.0	−57°.5→−27°.5
649	010°.0	−57°.5→−87°.5
651	060°.0	−57°.5→−27°.5
659	010°.7	−57°.5→−87°.5

The best solution is achieved with f_{deg} and p_{deg} equal 3. The accuracy of the final astrometric solution is of the order of what was expected. For most of the stars, the residuals are less than ∼1 arcsec (see figure 6).

With regard to the plate parameters we note that the scaling factors are not equal in J and K but are almost constant in each channel. The rotation angles seem to depend on the telescope position.

Strip	J		K	
Number	scale	angle	scale	angle
601	0.9831	0°.044	0.9838	0°.058
605	0.9835	0°.090	0.9838	0°.111
649	0.9834	0°.154	0.9825	0°.175
651	0.9834	0°.143	0.9835	0°.143
659	0.9841	0°.153	0.9838	0°.160

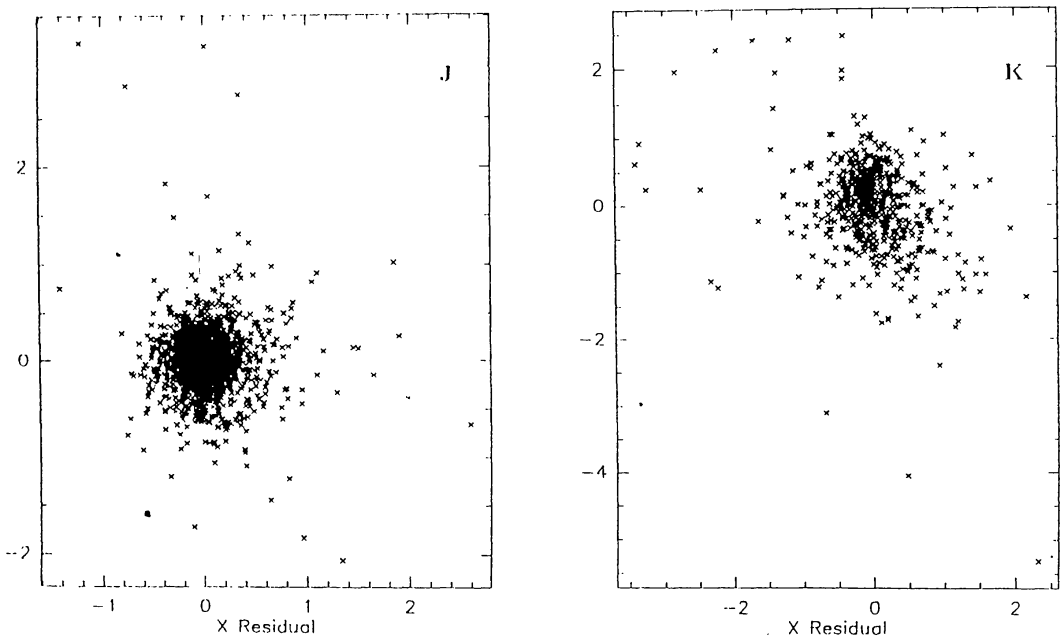

Fig. 6. As an example of the quality of the astrometric fit, one represents the residuals in Y position vs. the residuals in X for stars detected in strip 605 in J and K. The larger errors in K are due to the lower number of sources detected in this channel.

3.12. Use of the overlap region

The overall consistency of the process is tested by comparing the characteristics (positions, photometry, shape) of stars detected in the overlap region of two consecutive frames. For instance, comparison of their photometric parameters allows to estimate the photometric accuracy of our results as well as to check the pairing results. Hopefully, the average ratio of the photometric parameter is $\sim$1.01 and the 1σ error is less than $\sim$7% for reliable sources (Figure 7). Similar results are obtained in K.

3.13. Comparison of shape between overlap sources

The average quality of one strip can be investigated with the help of the parameters given by the extraction program for each detected sources such as their size, shape and position angle. For instance, bad seeing will increase the average size of the detected sources and defocussing will give a smaller average size of the detected sources in the central part of the frame than in the outer part.

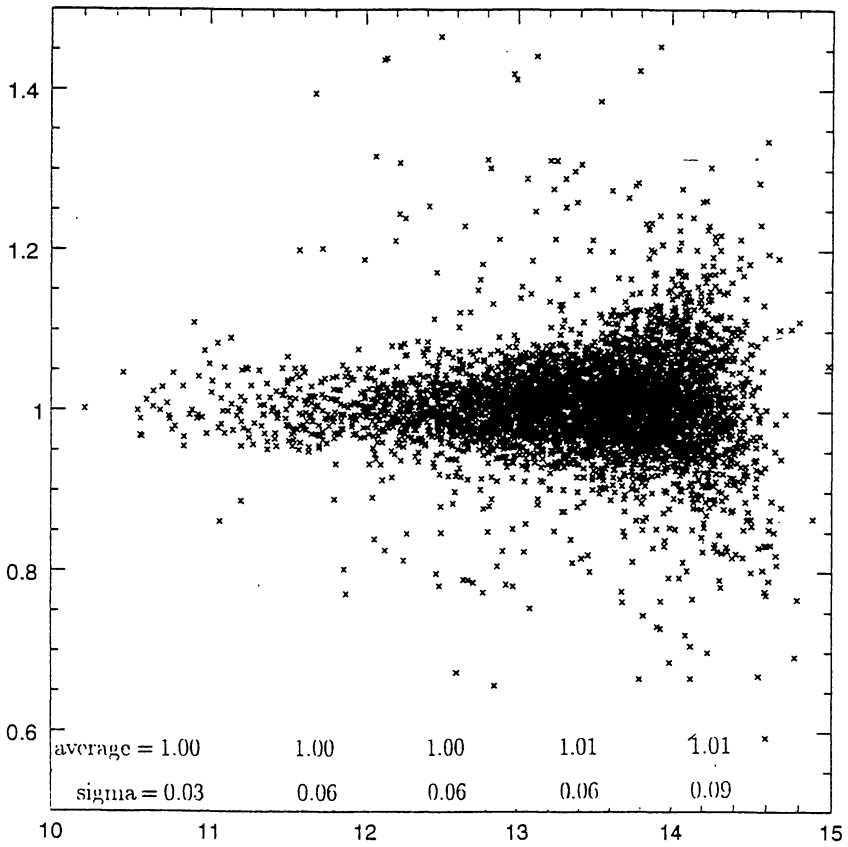

Fig. 7. Ratio of the photometric parameter of stars detected in the overlap region vs. -log of the photometric parameter (arbitrary unit) of sources of the upper frames. All sources are detected in 9 strips in J. The average and standard deviation are indicated for the unit bins

4. Photometric Calibration

DENIS will observe many standard stars during the survey and thus set a frame of reference of its own. To allow internal consistent derivation of the photometry and relate the DENIS photometry to other known reference frames we have build a catalog of standard stars. This section describes the creation of the standard star list and outlines the procedures planned to perform the photometric calibration of the DENIS survey.

4.1. The Standard Stars List

The list of standard stars used for DENIS has been divided into two parts, one for I and the other for J and K. The reason for this separation is that the expected limits (for detection and saturation) spread over a range of 4 mag. Furthermore, for historical reasons and, also, for technical reasons, I belongs to the optical range and, J and K, to the infrared range.

The pass–bands are specific to DENIS and do not correspond to any existing system. The filters were chosen for their imaging quality and for background minimization (K is centered at 2.15 μm, not 2.2 as usual). In addition, there are objectives (with 5 lenses), dichroics (1 for I, 2 for J & K) and a field lense in the light paths. Therefore, it is

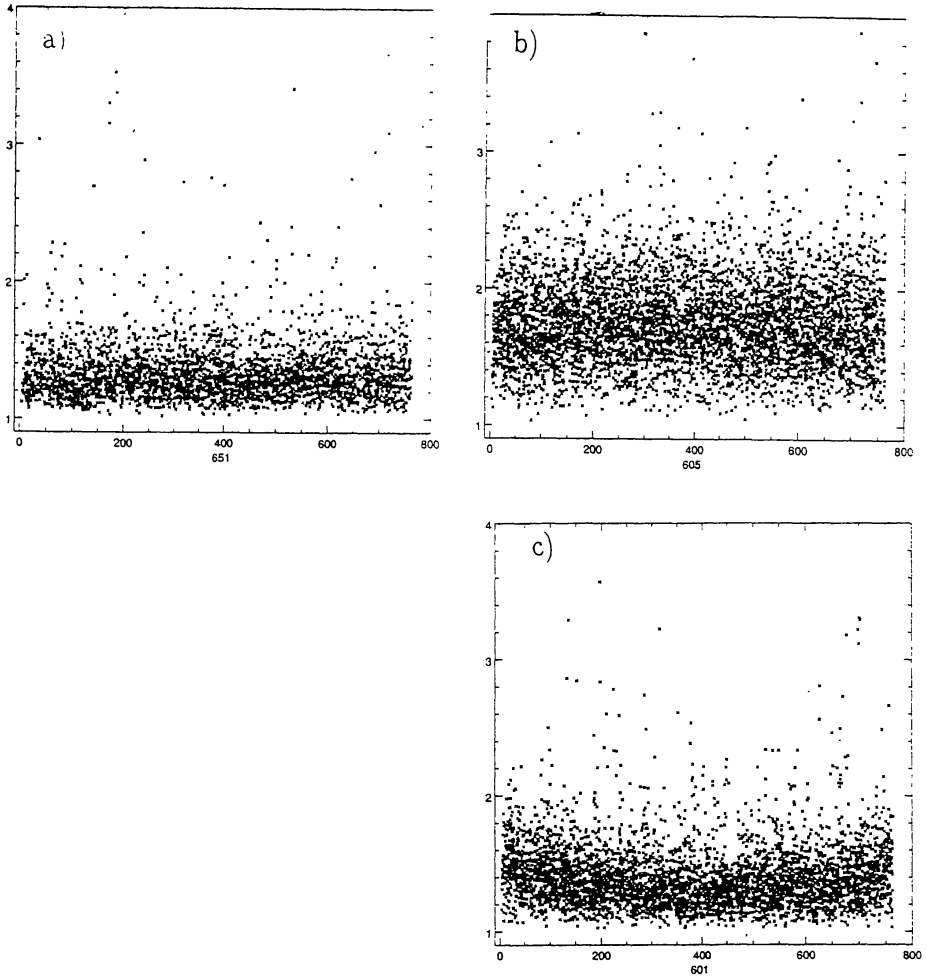

Fig. 8. The crosses represent the semi–major axis (a) as a function of the X position for each sources detected in: a) Strip 651 → observed with a good seeing (a∼1.34) b) Strip 605 → observed with a bad seeing (a∼1.75) c) Strip 601 → observed while the telescope is not well focussed (a∼1.41)

necessary to establish a specific photometric system for DENIS. This system could be developed ex–nihilo. However, from the beginning of the project, we felt necessary to tight the DENIS instrumental system to the other natural systems in use in the southern observatories.

For the J & K standards, we have compiled a list of standard stars from the lists in use at CTIO, ESO, MSSSO, SAAO and UKIRT. The stars that we have selected are well observed (so that they are confirmed to be non–variable) and have good positions and small proper motions (so that they can be recovered without ambiguity when automatic procedures are used). We have limited the number of bright stars that would saturate the NICMOS arrays by setting a limit at K = 5.0. The actual limits of saturation are at K ∼ 6.5 and J ∼ 8.0. However, there is some hope to recover photometric information on saturated stars by PSF fitting of the profile wings in the saturated images. How well this works and what the actual gain will be in dynamics is still controversial.

The present list contains 175 stars and is available publicly through one of the WWW DENIS servers (`http://denisexg.obspm.fr`). This list is not definitive and

will certainly evolve when new or revised standard lists become available. Also, it is expected that in the course of the survey some I standards which are bright enough will appear to be usable as J & K standards.

4.2. Observational procedure (SURVEY)

The southern sky will be covered by about 5000 strips of 12 arcmin. $\times$ 30°. In general, a strip does not contain any standard star. It is foreseen to observe at least one J & K and one I standard star between strips. Every star will be set on 8 different positions with respect to the detector which are arranged on a quasi–octogonal pattern of side $\sim$ 150 arcsec. The sky background will be derived from these photometric exposures by median filtering. The flat field will be taken from the closest strip(s). Dark exposures will be acquired together with the 8 photometric exposures. During the normal survey nights, it is expected that the number of observed standard stars (10 to 12 for each sub–set) will not be sufficient to derive the atmospheric extinction coefficients. For survey nights we interpolate the extinction coefficients between photometric nights and only derive instrumental zero-points. Checks will be performed to verify the photometric quality of the nights.

The data acquisition software provides the observer with estimated on-line magnitudes that can be used to check the quality of the night.

4.3. Observational procedure (Nights dedicated to photometry)

Some nights will be devoted to photometric calibration. The primary goal of these nights will be to derive atmospheric extinction coefficients and the instrumental responsivity. As the coefficients are expected to suffer seasonal variations, the photometric nights have to be spread over the year and over the whole length of the survey. We plan to concentrate them around the full Moon periods, because then the scattered light is expected to limit the performances in I. As in classical photometry, groups of rising and declining stars will be followed during the night. Then, from these nights the DENIS photometric system will be established.

The extinction coefficients and instrumental parameters will be determined through a least squares solution technique that may be based on a multi night approach. We will simultaneously solve the night's extinction coefficients for all stars per night, possibly for different nights too. This multi-night solution method will be used in a 'sliding window' technique, but will culminate at the end of the survey into a circle closure with a least square solution applied on all photometric data at once.

Recent experience has shown that about 60 photometric sequences (8 exposures + 1 dark) can be done during a photometric night. As this experience corresponds to summer nights, this should be a lower limit. Also, we expect to increase the efficiency of the photometric program.

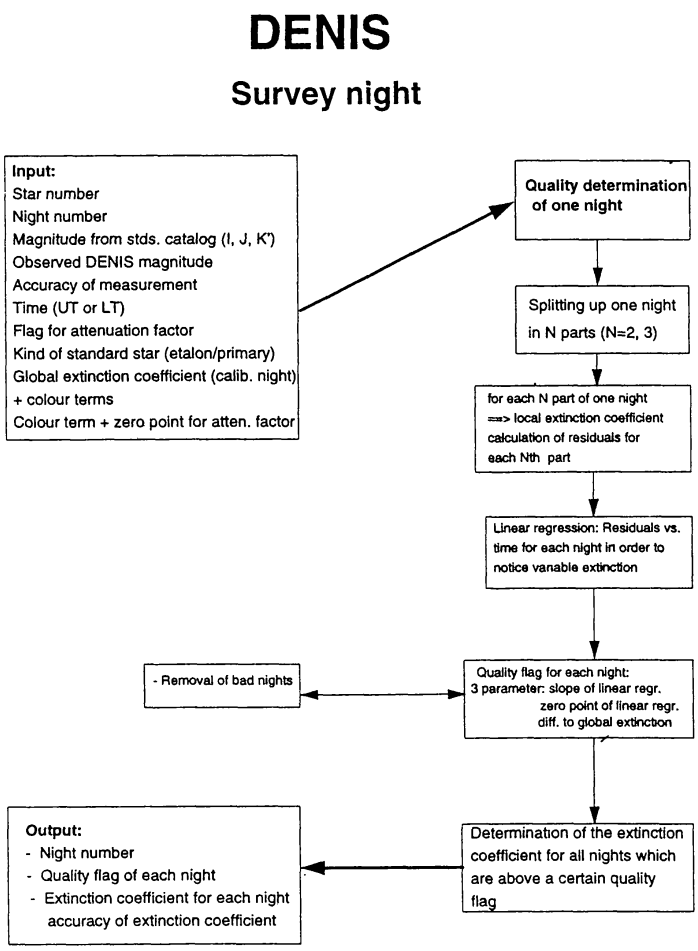

Fig. 9. Schematic view of the Survey night photometric calibration procedure

4.4. Side products of the photometric observations

During the length of the survey, and considering only the photometric nights, an infrared standard will be observed $\sim$ 40 times or more. In addition, from the survey nights, they should be observed typically 25–30 times.

¿From the photometric observations of standard stars defining the natural systems in use in other observatories, it will therefore be possible to derive the transformations between the DENIS system and these other systems.

Another side product comes from the fact that a field of $\sim$ 3 arcmin. $\times$ 3 arcmin. around each standard star is observed repeatedly with DENIS. Each photometric sequence yields 8 exposures; furthermore, each field should be observed $\sim$ 40 times or more during 4 years. It should be possible to reach much deeper limits in these fields than in the rest of the sky. As they are centered on a DENIS standard, they should be well–calibrated. Also, in these fields, it will be possible to select non–variable stars appropriate for photometric calibration; in general, these stars will be much fainter than the DENIS standards and suitable for large telescopes. Conversely, variability studies with a dense sampling over a period of 4 years will be possible. Eventually, stars with significant proper motion ($\geq$ 0.5"/year) could be found. However, as the fraction of the

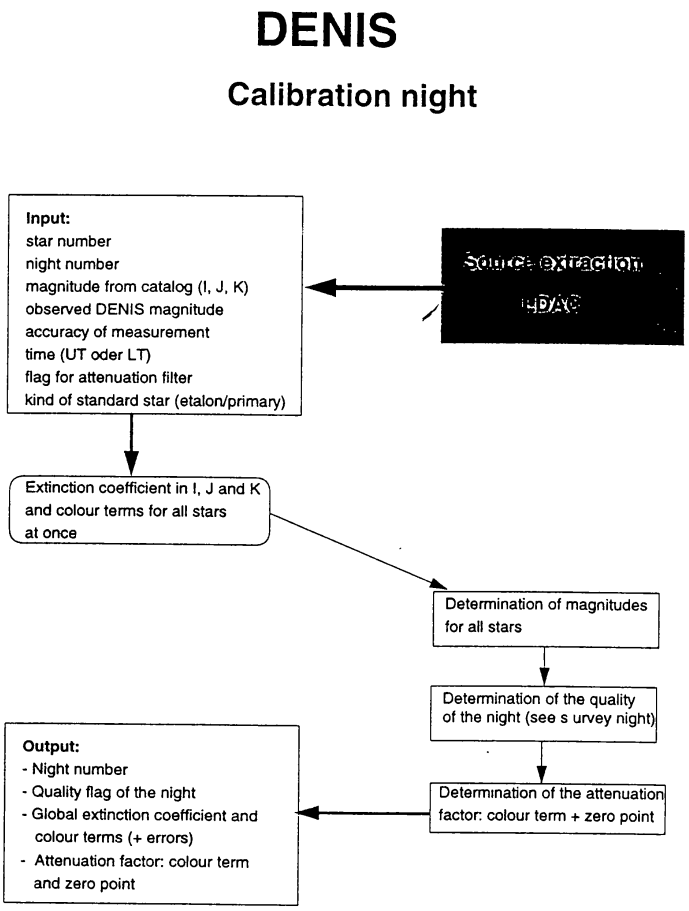

Fig. 10. Schematic view of the photometric (multi-)night calibration procedure

sky covered by these fields is around $175 \times 6\ 10^{-7}$ strd or 10^{-4} strd, the probability of finding new stars with large proper motion is low.

Acknowledgements

DENIS is the result of the collaboration of many researchers, engineers and technicians in a number of European Institutes and of the European Southern Obsevatory who are all warmly thanked. It would be impossible to quote here all the names of those who have contributed to the success of DENIS, but we are particularily indebted to J. C. Renault, the project manager, L. Capoani, S. Pau, and P. Rabou for the design and implementation of the camera, and to R. Vega for his efficient as the night assistant assigned by ESO to assist our Operations team. DENIS is partly funded by the SCIENCE and Human Capital and Mobility plans of the European Commission, the French Ministery of Education and Research (MESR), Centre National de la Recherche Scientifique (CNRS), and Institut National des Sciences de l'Univers (INSU), the State of Baden–Wurttemberg in Germany, the Spanish DIGICYT, the Netherlands Astronomical Expertise Center, the Italian Consiglio Nazionale delle Ricerche (CNR), the Austrian Fonds zur Forderung des

wissenschaftlichen Forschung und Bundesministerium fur Wissenschaft und Forschung, the Brazilian Fundation for the development of Scientifical Research of the State of Sao Paulo (FAPESP) and the Hungarian OTKA grants F-4239 and F-013990, and the ESO C& EE grant A-04-046.

References

Borsenberger, J, 1995, this Conference
Deul, E.R., 1994, ESO ST-ECF Data Analysis Workshop,
Epchtein. N, 1994, The DENIS Blue Book
Epchtein. N., (+25 authors), 1994, *Astrophys. Space Sci.* **217**, 3
Golub G.H. and Van Loan C.F., 1989, Matrix computations, The Johns Hopkins University Press, Baltimore.
Høg E. et al.: 1991, *Astrophys. Space Sci.* **177**, 109
Jenkner, H., Lasker, B.M., Sturch, C.R., McLean, B.J. Shara, M.M., Russel, J.L., 1990, *Astron. J.* **99**, 2081
Kimeswenger, S., Kienel, C., 1994, *Astrophys. Space Sci.* **217**, 23
Taff L.G. et al.: 1990, *Astrophys. J. Lett.* **353**, L45